Bound-state evolution in curved waveguides and quantum wires

O. Olendski
Atomic and Molecular Engineering Laboratory, Belarussian State University, Skarina Avenue 4, Minsk 220050, Belarus

L. Mikhailovska
Department of Higher Mathematics, Military Academy, Minsk 220056, Belarus

(Received 4 April 2002; published 26 July 2002)

A theoretical study of a waveguide with a uniformly curved section is presented within the envelope function approximation. Utilizing analytical solutions in each part of the waveguide, exact expression of the scattering matrix of the system is derived. Based on it, a conductance of the waveguide is calculated for the wide range of the bend angle and radius. It is shown that a quasibound state formed as a result of the bend, at some critical parameters of the curve becomes a true bound state with infinite lifetime. It has its degenerate continuum counterpart, but does not interact with it. As a result of a constructive resonant interference in the bend, dip in the conductance, which is an essential property for the noncritical values, vanishes with full transmission being observable instead. Mathematical and physical interpretation of these results is given, and characteristic features of the critical parameters are discussed. Comparison with quantum waveguides with other types of nonuniformity is performed.

DOI: 10.1103/PhysRevB.66.035331 PACS number(s): 73.63.Nm, 03.65.Ge, 73.22.Dj, 84.40.Az

I. INTRODUCTION

Sophisticated modern growth nanotechnologies allow one to build up structures where carrier motion may be confined in one, two or three dimensions. Quantum structures, where an electron is free to move between two parallel layers but not in the direction perpendicular to them are called quantum quasi-one-dimensional (Q1D) waveguides. The discovery of conductance quantization in such quantum channels[1,2] stimulated a lot of theoretical and experimental attention to their transport properties, especially when a uniformity of the waveguide is broken. It was shown that a quantum dot embedded into the waveguide significantly alters its conductance, leading to the new dips and resonances which are absent without the scatterer.[3–8] These resonances were attributed to the appearance of the discrete levels in the continuum and their interaction with the continuum states. A bend presents another type of nonuniformity frequently met with in the waveguides. Investigation of its influence on the transport properties of the quantum channels received extensive consideration recently. It was discovered that a bend in the uniform waveguide leads to the bound states spatially localized in the bent region with energies below subband thresholds.[9–12] These levels interfere destructively with the propagating modes resulting in the dips of the conductance.[13–16] In a sense, this makes them similar to the discrete levels induced by the impurity potential. However, there are some significant differences between them. First, shapes of the conductance resonances in both cases are not the same; and, more importantly, origins of these states are different. In the case of impurity an attractive potential creates additional levels while for the bent waveguides the extra space in the bend accommodates electrons with de Broglie wavelength exceeding the cutoff wavelength of the above lying subband. Specific value of this de Broglie wavelength (and, accordingly, bound-state energy) is uniquely determined by the parameters of the bend. In particular, for the sharply bent waveguides the number of the bound states for each subband changes from one to infinity when the bend angle increases from zero to 180°, and for the curved waveguide, i.e., a structure with a constant cross section, a second bound state appears only for the physically irrelevant bend angle larger than 5π.[15]

We want to note that the problem of the bent waveguide possesses quite universal generality applicable in many areas of physics and chemistry. For example, in Ref. 17 one of the models of quark confinement is reduced to the problem of wave interference in a two-dimensional right-angle channel. It was also used for the investigation of chemical rearrangement processes.[18]

Long before nanoelectronics, wave propagation in bent waveguides was widely discussed in radiophysics and electrodynamics. From a point of view of mathematical physics, both electron transmission through the quantum wire and electromagnetic wave propagation along the metallic waveguide are described by the same type of second-order differential equation for scalar fields in two dimensions, namely, by the Helmholtz equation. Extensive bibliography of the electromagnetic waves propagation along the bent structures dating back to the end of the nineteenth century may be found in Refs. 19–21. As far back as 1969, Bates[22] had shown that the reflection coefficient of the junction between a straight and a curved radio waveguide is expected to increase sharply in the immediate neighborhood of cutoff frequencies. This was explained by the fact that a mode may be propagating in the curved part while still cut off in the straight section or vice versa, depending on the wave polarization—clear analogy to the bound states in bent quantum wires (see also Ref. 23). However, at that time, computational difficulties precluded a detailed analysis of this phenomenon. Miscellaneous aspects of the bent metallic waveguides continue to attract attention of radio scientists.[24]

In the present paper we return to the problem of the waveguide containing uniformly curved section, with two main aims in mind. First, within an effective-mass approximation and a noninteracting electron picture we present an exact form of the scattering matrix of the system. Exact analytical solutions are developed in each region and matched on the boundaries between them. In particular, in the bend an azimuthal component of the wavefunction is expressed through trigonometric functions with noninteger angular momentum. Accordingly, the radial part contains a combination of the Bessel functions with non integer index, which is either real or purely imaginary. Real indices correspond to the modes propagating inside the curve, and imaginary ones describe the evanescent states. Comparative analysis between this and other known approaches is given. Among others, one of the advantages of our method lies in the fact that, matching wave function at the junctions, one can derive formally an exact expression for the scattering matrix $\mathbf{S}(E)$ which is a function of the incident electron energy E. Its knowledge allows one to calculate the two-probe total conductance G,[25]

$$G(E)=\frac{2e^2}{h}\sum_{nn'}\frac{k_{n'}}{k_n}S^*_{nn'}S_{nn'}, \tag{1}$$

where k_n is the electron wave vector of the channel n and the scattering matrix element $S_{nn'}$ defines the probability of the electron scattering from channel n to n'. Sum in Eq. (1) runs over all open channels.

Secondly, studying the conductance G, we concentrate on the analysis of the resonance dip location E_{min} and, mainly, the resonance half width Γ as functions of the parameters of the bend. It is known that a dip in the conductance is due to the interaction of the quasibound state raised into the continuum with its degenerate continuum counterpart. Accordingly, the value of $\hbar/\Gamma$ defines the lifetime of the quasibound state. We find out that under some values of the bend parameters the value of Γ shrinks to zero, which corresponds to the stable state—the state with infinite lifetime. Physically this state is stable since under these very special conditions it does not interact with the continuum, accordingly, there is no reason for it to decay. Constructive interference in this case causes the dip in the conductance to disappear. We also draw parallels between our model and the recently studied collapse of the Fano resonances in the Q1D waveguide with embedded quantum dot. We find a very strong similarity between these two cases indicating the same nature of the coherent phenomena in both configurations.

The paper is organized as follows. In Sec. II our model is presented and a necessary formulation of our method is given. Several advantages of this approach are also briefly discussed. Section III is devoted to the presentation and detailed physical interpretation of the calculated results. Summary of the results is provided in Sec. IV. In the Appendix we write the explicit form of the scattering matrix for our system.

II. MODEL AND FORMULATION

We consider a Q1D quantum waveguide of width d, which contains a bend of inner radius ρ_0 and angle ϕ_0 (Fig. 1). Hard wall boundary conditions and a uniform curvature of the circular bend are assumed for simplicity. Straight parts of the waveguide are assumed to be infinitely long. Magnetic field is assumed to be zero, but, similar to Refs. 16 and 26, may be included into consideration at the later stage. Throughout our analysis we also impose a ballistic regime of the electron transport.

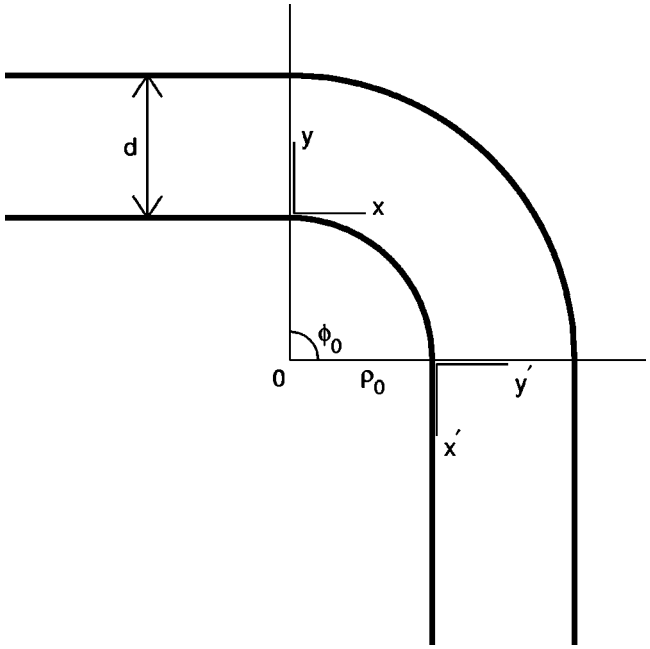

FIG. 1. Schematic picture of the curved quantum waveguide we study in this paper. Bend radius and angle are ρ_0 and ϕ_0, respectively. Width of the waveguide is a constant d. Local coordinate systems (x,y) and (x',y') for the straight arms are also shown.

The single-particle Schrödinger equation describing electron wavefunction, reads

$$-\frac{\hbar^2}{2m^*}\Delta\Psi(\mathbf{r})=E\Psi(\mathbf{r}) \tag{2}$$

with the wavefunction Ψ vanishing at the boundaries of the quantum wire. m^* in Eq. (2) is the effective electron mass. As Fig. 1 shows, the geometry of the system dictates a natural choice of the two-dimensional radius vector $\mathbf{r}$ in terms of rectangular coordinates (x,y) or (x',y') in the straight parts of the waveguide and in terms of polar coordinates (ρ,ϕ)—in the bend. We will measure all distances in units of the waveguide width d. Accordingly, all energies will be measured in units of $\pi^2\hbar^2/(2m^*d^2)$. In turn, in these units the wave vector of the channel n becomes $\pi E^{1/2}$ and its longitudinal component $k_n=\pi\sqrt{E-n^2}$. We also accept a unit of time as $2m^*d^2/(\pi^2\hbar)$.

To the left of the bend, solution to Eq. (2) is

$$\Psi(x,y)=\sum_{n=1}^{\infty}[A_n\exp(i\pi\sqrt{E-n^2}x) + B_n\exp(-i\pi\sqrt{E-n^2}x)]\chi_n(y) \tag{3}$$

with

$$\chi_n(y) = 2^{1/2}\sin(n\pi y). \tag{4}$$

After the bend one has

$$\Psi(x',y') = \sum_{n=1}^{\infty} C_n \exp(i\pi\sqrt{E-n^2}x')\chi_n(y'). \tag{5}$$

In Eq. (3) the terms with coefficients A_n describe the waves incident upon the bend, the terms with coefficients B_n are the modes reflected from (if $E>n^2$) or localized near it (for $E<n^2$). In the same way, in Eq. (5) the terms with positive $E-n^2$ are the modes propagating away from the curved area, and those with $E-n^2<0$ are the states bounded by it.

In a particular case, for A_n being a Kronecker symbol: $A_n=\delta_{nm}$, $m=1,2,\ldots$, due to the conservation law the following relation holds for the energies E such that $E>m^2$:

$$\sum_{n=1}^{\infty}\left(\frac{E-n^2}{E-m^2}\right)^{1/2}(|C_n|^2+|B_n|^2)\,\theta(E-n^2)=1. \tag{6}$$

$\theta(x)$ in Eq. (6) is a step function, and terms $[(E-n^2)/(E-m^2)]^{1/2}|C_n|^2$ and $[(E-n^2)/(E-m^2)]^{1/2}|B_n|^2$ are, respectively, current transmission and reflection probabilities between subbands m and n.

Inside the bend, in the polar coordinate system with the polar point coinciding with the center of the bend and the polar axis being the vertical junction between the straight and bent parts of the waveguide, solution of the Schrödinger equation reads

$$\Psi(\rho,\phi) = \sum_{n=1}^{\infty} R_n(\rho)[D_n\sin(\nu_n\phi)+F_n\cos(\nu_n\phi)] \tag{7}$$

with $R_n(\rho)$ being a radial part of the wave function

$$R_n(\rho) = Y_{\nu_n}(\pi E^{1/2}\rho_0)J_{\nu_n}(\pi E^{1/2}\rho) - J_{\nu_n}(\pi E^{1/2}\rho_0)Y_{\nu_n}(\pi E^{1/2}\rho). \tag{8}$$

Here $J_\nu(x)$ and $Y_\nu(x)$ are Bessel functions of the first and second kind, respectively,[27] and ν_n is the nth root of the equation

$$Y_\nu(\pi E^{1/2}\rho_0)J_\nu(\pi E^{1/2}(\rho_0+1)) - J_\nu(\pi E^{1/2}\rho_0)Y_\nu(\pi E^{1/2}(\rho_0+1)) = 0. \tag{9}$$

The left-hand side of Eq. (9) is considered as a function of variable ν which is the index of the Bessel functions with all other parameters fixed. Accordingly, contrary to the system with circular symmetry, in our case ν_n are not real integers. It is known[19,28] that the solutions of Eq. (9) are discrete and countably infinite, and only a finite number of the zeros are real, the remainder being purely imaginary. As Eq. (7) shows, real zeros are naturally associated with the modes propagating inside the bend, and imaginary values describe the evanescent waves.

Since Bessel functions are a natural mode for the uniformly curved guide, representation of the radial part of the solution in the form given by Eq. (8) is advantageous compared to other methods such as, for example, expansion in the trigonometric basis set[29] or discretization of the Schrödinger equation by nonrectangular mesh.[30] In particular, it allows one to directly determine the number of modes propagating inside the bend. Namely, from the properties of the Bessel functions[27] it follows that if $x_l^{(0)}\leqslant\pi E^{1/2}<x_{l+1}^{(0)}$ with $x_l^{(0)}$ being l-th root of equation

$$Y_0(x\rho_0)J_0(x(\rho_0+1)) - J_0(x\rho_0)Y_0(x(\rho_0+1)) = 0, \tag{10}$$

then the total number of the propagating modes in the bend equals l. Roots of Eq. (10) are well known and can be found, e.g., in Refs. 27 and 31. For the electromagnetic waveguides, a comparative discussion of the Bessel and trigonometric basis sets for different kinds of the bends was presented in Ref. 32.

At the junctions we have the following relations between the three coordinate systems (x,y), (ρ,ϕ), and (x',y'):

$$(x=0,y)\Leftrightarrow(\rho_0+y,\phi=0), \tag{11}$$

$$(x'=0,y')\Leftrightarrow(\rho_0+y',\phi=\phi_0), \tag{12}$$

$$\left.\frac{\partial}{\partial x}\right|_{x=0}\Leftrightarrow\left.\frac{1}{\rho_0+y}\,\frac{\partial}{\partial\phi}\right|_{\phi=0}, \tag{13}$$

$$\left.\frac{\partial}{\partial x'}\right|_{x'=0}\Leftrightarrow\left.\frac{1}{\rho_0+y'}\,\frac{\partial}{\partial\phi}\right|_{\phi=\phi_0}. \tag{14}$$

Keeping this in mind, one can match the wave function and its derivative in the straight and bent parts of the waveguide. This leads to a system of equations for determining coefficients A_n, B_n, C_n, D_n, and F_n. Eliminating from them B_n, D_n, and F_n, it is possible to arrive at the relation between infinite vectors **A** and **C**,

$$\mathbf{C}=\mathbf{S}\mathbf{A}. \tag{15}$$

An explicit form of the scattering matrix **S** is given in the Appendix. Since its form is a quite complicated one, we do not extract any analytical information from it, performing instead a direct numerical evaluation of the conductance G from Eq. (1).

III. RESULTS AND DISCUSSION

In the subsequent analysis we confine our attention to the fundamental propagating mode only with $1\leqslant E\leqslant 4$. In this case only one propagating channel exists, and the most characteristic features of the discussed phenomena are not obscured by the interference between different propagating modes. Equation (1) then becomes

$$G(E) = \frac{2e^2}{h}|S_{11}|^2. \tag{16}$$

Also, we do not take into account the physically irrelevant angles larger than 180°.

Figure 2 shows the normalized conductance $G^*=G/(2e^2/h)$ as a function of the Fermi energy E for the bend

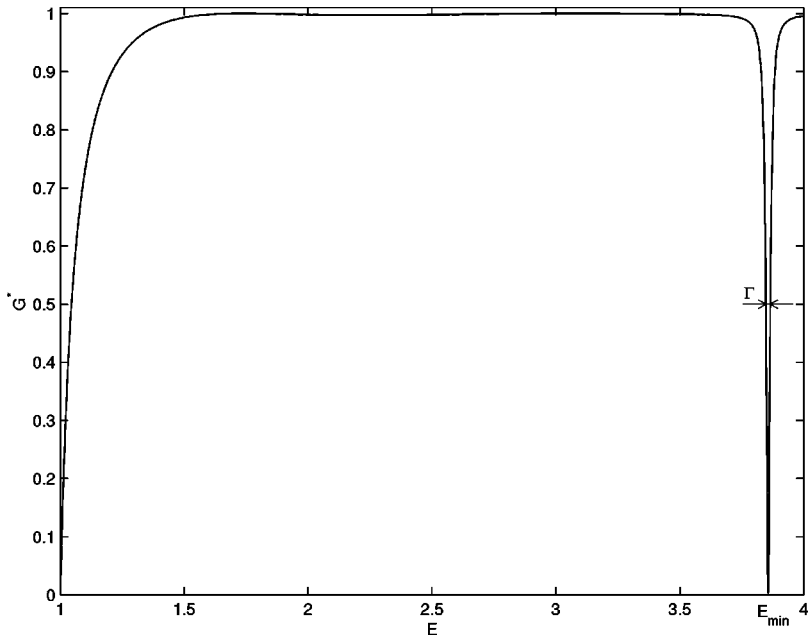

FIG. 2. Conductance $G^*=G/(2e^2/h)$ as a function of the Fermi energy E for $\rho_0=0.001$ and $\phi_0=180°$. Resonance is characterized by its zero transmission location E_{min} and the half width Γ which together form a complex energy of the quasibound level $E_{qb}=E_{min}-i\Gamma/2$.

radius $\rho_0=0.001$ and the bend angle $\phi_0=180°$. It is seen that immediately after the lower threshold, from zero the conductance rapidly grows with energy and very soon approaches values very close to unity. Another remarkable feature of the energy-conductance relation is the pronounced dip in the conductance near the next threshold. Namely, as Fig. 2 shows, close to the next subband conductivity drops abruptly, at energy E_{min} reaches minimum equal to zero, and then rapidly grows again. This dip in the transmission is explained by the formation, in the circular part, of a localized mode with energy below the threshold value. The bend provides an additional space where a particle can dwell with its momentum smaller compared to the straight sections. This localized state interferes destructively with the continuum states causing the conductance to drop, and at E_{min} we have a complete interference blockade of the electron transport. Such localized level is split off from each subband, however, only the level split off from the fundamental mode is a true bound state with its wave function in the straight parts being an evanescent exponent in the longitudinal direction. As we mentioned before, we assume the infinite length of the straight waveguides, thus forbidding tunneling of this level out of the bend into the leads. All levels splitting off from the higher-lying subbands, due to their interaction with the continuum are, in general, quasibound states, or resonances, which may escape into the infinity. Energies E_{min} at which zero transmission occurs are functions of the radius ρ_0 and the angle ϕ_0. They are shown in Fig. 3 as a function of the bend angle ϕ_0 for several values of ρ_0. It is seen that quasibound state energy monotonically decreases with the bend

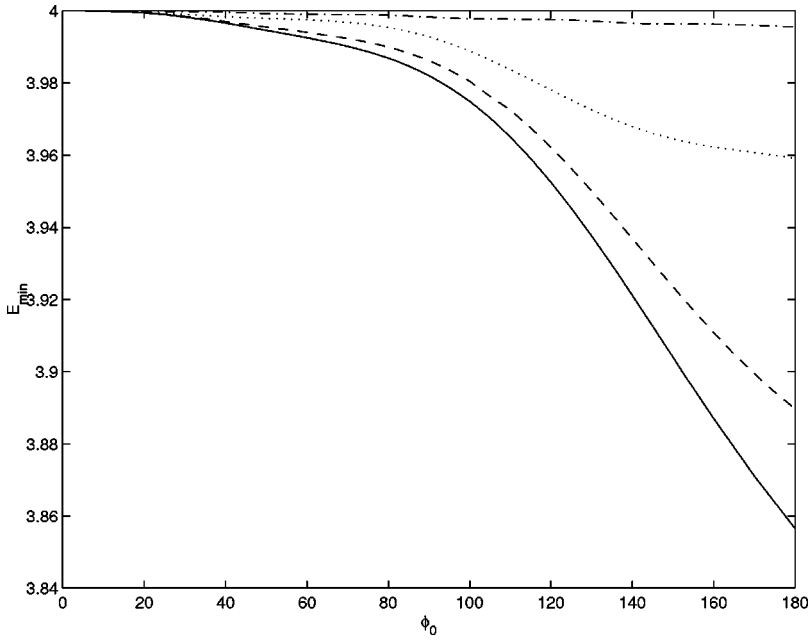

FIG. 3. Energy E_{min} as a function of the bend angle ϕ_0 for several values of the radius ρ_0: the solid line is for $\rho_0=0.001$, the dashed line is for $\rho_0=0.01$, the dotted line is for $\rho_0=0.1$, and the dash-dotted line is for $\rho_0=1$.

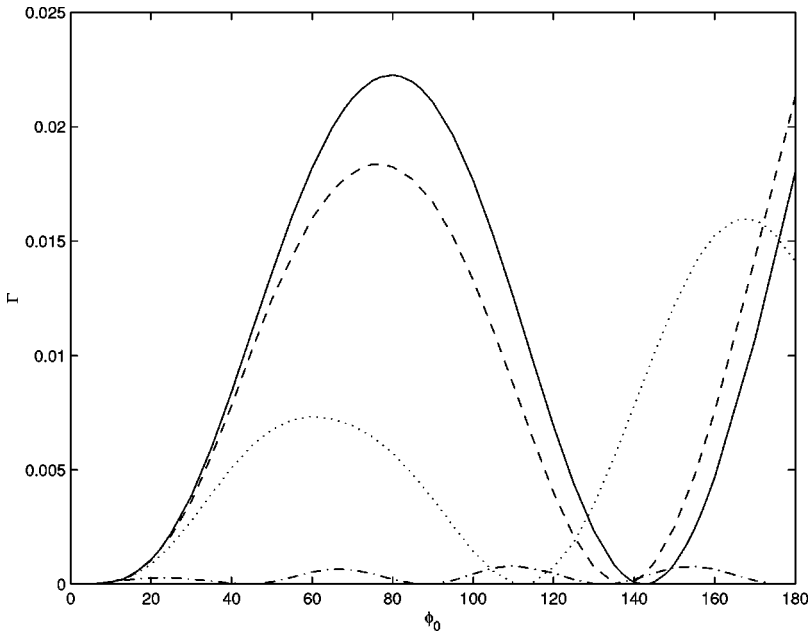

FIG. 4. Half width Γ as a function of the bend angle ϕ_0 for several values of the radius ρ_0.The same convention as in Fig. 3 is used. Curve for $\rho_0=1$ has four zero minima on ϕ_0 axis (excluding point $\phi_0=0$).

angle growing. Also, E_{min} deviates stronger from the higher-lying subband threshold for the smaller radius ρ_0. This is quite understandable since a larger bend angle and a smaller radius present a larger perturbation to the electron motion in the uniform waveguide causing quasibound state energy to deviate stronger from the unperturbed values.

When one talks of the resonant scattering, another very important parameter to discuss is the half width of the resonance Γ. This value is shown by the arrows in Fig. 2. In fact, we can say that a quasibound state has a complex energy E_{qb},

$$E_{qb}=E_{min}-i\Gamma/2. \tag{17}$$

Γ determines the lifetime of the quasibound state τ by

$$\tau=\frac{1}{\Gamma}. \tag{18}$$

Figure 4 shows the half width Γ as a function of the angle ϕ_0 for several values of ρ_0. It is seen that Γ increases together with the moderate values of the bend angle, reaches maximum (for example, for $\rho_0=0.01$, $\Gamma_{max}=0.018\,37$ is reached at $\phi_0\simeq 76°$) and then decreases to minimum of *zero* after which it grows again. Depending on ρ_0, such situation can be repeated a few times. For example, for $\rho_0=1$ one can observe four minima of Γ. Zero magnitude of the half width in the minimum means that the corresponding level at these critical parameters turns into the true bound state with infinite lifetime, as it follows from Eq. (18). Thus, under these special conditions transformation from the quasilocalized state to the true bound level takes place.

To explain this, we write the most general form of the wave function of the quasibound level in one of the straight parts of the waveguide,

$$Q_1\exp(-i\pi\sqrt{E-1}x)\chi_1(y) + \sum_{n=2}^{\infty} Q_n\exp(\pi\sqrt{n^2-E}x)\chi_n(y) \tag{19}$$

(recall that we confine our consideration to the fundamental mode only). Similar expression can be written for the other arm as well. Magnitude of $|Q_1|^2$ defines the escape rate of the corresponding state. In fact, it is proportional to the half width. Generally, when it is not zero, there is a nonzero probability of the electron escape to the infinity. However, if somehow we create conditions such that $Q_1\equiv 0$, then there is no channel for the electron to tunnel out of the bend since its wave function does not contain a plane-wave component now, but instead exponentially vanishes in the straight arms. Thus, we have a true bound state. Using an analogy with elementary quantum mechanics, we can call this level *first excited* true bound state, and the level split off from the fundamental mode—*ground* true bound state. They are similar, since particles in both of them are trapped by the bend and (for the infinite arms) cannot perform infinite motion away from it. However, there are some considerable differences between these two states. First, a ground true bound state always exists for any magnitude of the bend radius and the angle. And, as we saw above, the excited true bound state appears only under very special conditions when the coherent resonant phenomena in the bend cancel out the plane waves in the straight arms. Second, the ground bound state is split off from the lowest subband threshold and, as such, does not have a degenerate continuum counterpart. In its turn, excited true bound state still is degenerate with the continuum. However, contrary to the quasibound case, this degeneracy now does not cause any interaction between them. Instead, a constructive interference in the bend now erases the dip on the energy-conductance dependence, as can be seen from Fig. 5. It shows G^* as a function of the Fermi energy for the case of $\rho_0=0.01$ and $\phi_0=136.90°$, i.e., when

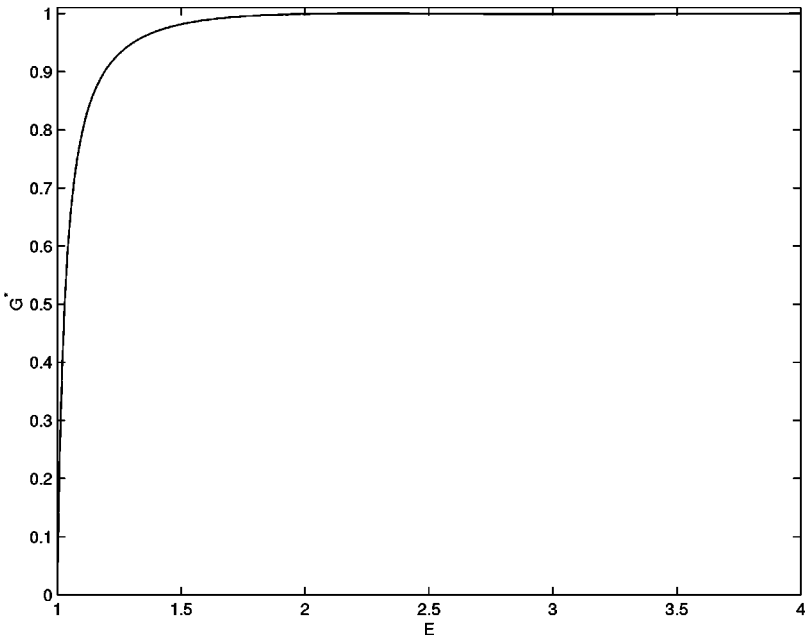

FIG. 5. Conductance G^* as a function of the Fermi energy E for $\rho_0=0.01$ and $\phi_0=136.90°$. There is no dip in the transmission for these critical parameters of the bend.

the corresponding Γ turns to zero in Fig. 4. Instead of the dip we see the resonant tunneling through the bend with transmission in the wide range of energy being practically indistinguishable from the unity. The only influence of the bend on the conductance in this case is the zero transmission at $E=1$ and its quick approach to unity with the energy growing from the subband threshold. Thus, a bent waveguide is added to the class of quantum physical systems,[8,33] where a bound state in the continuum appears as a very special solution of the Schrödinger equation.

Since the disappearance of the dip in the conductance is caused by the wave interference in the bend, one can qualitatively explain the different number of the minima for the different radii in Fig. 4. As all the resonances we consider here take place near the second subband threshold, in the first approximation we can say that the longitudinal de Broglie wavelength $\lambda_{min}=2/(E_{min}^{1/2}-1)$ of the bound state is independent of ρ_0 and ϕ_0: $\lambda_{min}\approx 2$. On the other hand, for the larger ρ_0 length of the arc $(\rho_0+1/2)\phi_0$, which roughly determines the resonant length, is also larger, and, accordingly, the first resonant condition when only one half of the wavelength λ_{min} is accommodated by the bend, is achieved for the smaller angle. For the sufficiently large ϕ_0 the second resonant condition can be realized when the bend can accommodate one full wavelength λ_{min}. As Fig. 4 shows, for the bend radii $\rho_0\leqslant 0.1$ it occurs at the angles $\phi_0\geqslant 180°$, however, for the large radii higher-order resonances can be achieved a few times in the physically interesting range of $0°\leqslant\phi_0\leqslant 180°$.

Finally, we want to compare the above presented results with the study of the collapse of the Fano resonances in the straight Q1D waveguide with embedded quantum dot.[8] We see many similarities between these two cases. Both waveguide nonuniformities raise the quasibound states into the continuum and, as a result, form their corresponding peculiar resonances; in both cases, by changing the geometrical parameters of the waveguide perturbation, this resonance can be erased or substituted by the resonant tunneling with absolute transparency through the obstacle, and a quasibound state can be transformed into the true bound level, which has it degenerate continuum counterpart. This strong similarity stems from the same physical origin of these effects, namely, from the coherent resonant phenomena in the nonuniformities of the waveguide.

IV. CONCLUDING REMARKS

We have considered the transmission properties of the Q1D waveguide with uniformly curved section in the wide range of the bend parameters. Expressing solutions of the wave equation in the bent part by the analytical functions allowed us to derive an exact expression for the scattering matrix **S**. It also allowed us to conveniently calculate transport properties of the structure. We have found that under some critical parameters of the curve, quasibound level in the bend transforms into the true bound state. Accordingly, as a result of a coherent resonant phenomena in a circular arc, a dip in the conductance typical for the noncritical parameters, disappears, turning into the full transmission resonant tunneling. These interference effects open up the possibility of controlling the transport properties of the waveguide by simple tuning of the geometry of its bend.

Only circular bends have been considered in this paper. The relevant geometrical parameters in this case are the bend radius ρ_0 and the bend angle ϕ_0. On the contrary, for the sharply bent waveguide the only factor affecting the transmission is the bend angle. Some comparative analysis of the sharply and circularly bent waveguides has been performed in Ref. 15. Because of the additional extra space in the corner of the sharply bent waveguide, it binds the electrons stronger with the bound-state energy being always lower than that for the circular bend. The other difference is the presence of many bound states below the fundamental threshold for the bend angle close to 180°. However, all other physical effects described here for the curved structures

such as the quasibound state transformation into the true bound level with its degenerate continuum counterpart, should be present in the sharply bent waveguides as well.

The first experimental confirmation of the existence of the bound states in the bent guiding structures has been obtained by the use of the transverse-electric mode microwaves in metallic waveguides.[14,15] The same technique may be used for detecting the bound states discussed above and for mapping their spatial localization.

A few possible continuations of the present work are worth mentioning. First, we found a very strong correspondence between our excited true bound state and the collapse of the Fano resonances in the Q1D waveguide with embedded quantum dot. It is intriguing to find out how these two nonuniformities—bend and embedded attractive scatterer—will interact with each other.

Next, as we mentioned earlier, the magnetic-field influence on the bent waveguides was calculated by several authors. It was shown[16] that applied static magnetic field shifts upwards E_{min} and squeezes Γ. It is natural to wonder: what happens with excited true bound states when a magnetic field is taken into the consideration?

Throughout the paper we assumed the hard-wall boundary conditions meaning that the fields do not penetrate outside the waveguide. It is a good approximation for the hollow metallic guiding structures. On the contrary, in the optical waveguides[34] and quantum wires with finite height barriers some part of the energy propagates outside the guide core. Accordingly, when such a structure is bent, guided along the structure energy is lost due to the radiation from the bend.[20,35,36] In its turn, the mode that was truly localized in the metallic waveguide becomes a quasilocalized state with finite lifetime with the additional possibility to leak out not only into the straight parts, but in the radial direction as well. Calculation of the amount of the bending loss and localized modes behavior in such structures is not only of fundamental theoretical interest, but also of a paramount applied technical significance. A phenomenal growth of the fiber optic communication industry insistently dictates further spatial reduction in the design of integrated optical circuits where many separate optical devices on a single chip are to be interconnected by the channels with bends. We are not aware of any results addressing quasibound state behavior in bends in the optical waveguides. This problem needs a special investigation.

APPENDIX

We provide here the exact expression for the scattering matrix,

$$\mathbf{S}=\{\mathbf{Q}_5(\mathbf{Q}_1-\mathbf{Q}_2\mathbf{Q}_4^{-1}\mathbf{Q}_3)^{-1}+\mathbf{Q}_6(\mathbf{Q}_2-\mathbf{Q}_1\mathbf{Q}_3^{-1}\mathbf{Q}_4)^{-1}\}\mathbf{Q}_7, \tag{A1}$$

where the infinite matrices $\mathbf{Q}_i$ $(i=1,2,3,4,5,6,7)$ have the following structure:

$$(\mathbf{Q}_1)_{nn'}=\nu_{n'}\left[\sum_{m=1}^{\infty}\left(\frac{1+i\pi\sqrt{E-m^2}}{1-i\pi\sqrt{E-m^2}}I_{mn}^{(3)}I_{mn'}^{(1)}\right)+I_{nn'}^{(4)}\right], \tag{A2}$$

$$(\mathbf{Q}_2)_{nn'}=\sum_{m=1}^{\infty}\left(\frac{1+i\pi\sqrt{E-m^2}}{1-i\pi\sqrt{E-m^2}}I_{mn}^{(3)}I_{mn'}^{(2)}\right)-I_{nn'}^{(5)}, \tag{A3}$$

$$(\mathbf{Q}_3)_{nn'}=\sin(\nu_{n'}\phi_0)(\mathbf{Q}_2)_{nn'}-\cos(\nu_{n'}\phi_0)(\mathbf{Q}_1)_{nn'}, \tag{A4}$$

$$(\mathbf{Q}_4)_{nn'}=\cos(\nu_{n'}\phi_0)(\mathbf{Q}_2)_{nn'}+\sin(\nu_{n'}\phi_0)(\mathbf{Q}_1)_{nn'}, \tag{A5}$$

$$(\mathbf{Q}_5)_{nn'}=\frac{1}{1-i\pi\sqrt{E-n^2}}[\sin(\nu_{n'}\phi_0)I_{nn'}^{(2)}-\nu_{n'}\cos(\nu_{n'}\phi_0)I_{nn'}^{(1)}], \tag{A6}$$

$$(\mathbf{Q}_6)_{nn'}=\frac{1}{1-i\pi\sqrt{E-n^2}}[\cos(\nu_{n'}\phi_0)I_{nn'}^{(2)}+\nu_{n'}\sin(\nu_{n'}\phi_0)I_{nn'}^{(1)}], \tag{A7}$$

$$(\mathbf{Q}_7)_n=4\sum_{m=1}^{\infty}\frac{i\pi\sqrt{E-m^2}}{1-i\pi\sqrt{E-m^2}}I_{nm}^{(3)}, \tag{A8}$$

and

$$I_{nn'}^{(1)}=2^{1/2}\int_0^1\frac{1}{\rho_0+x}\sin(n\pi x)R_{n'}(\rho_0+x)dx, \tag{A9}$$

$$I_{nn'}^{(2)}=2^{1/2}\int_0^1\sin(n\pi x)R_{n'}(\rho_0+x)dx, \tag{A10}$$

$$I_{nn'}^{(3)}=2^{1/2}\int_0^1(\rho_0+x)\sin(n\pi x)R_{n'}(\rho_0+x)dx, \tag{A11}$$

$$I_{nn'}^{(4)}=2^{1/2}\int_0^1R_n(\rho_0+x)R_{n'}(\rho_0+x)dx, \tag{A12}$$

$$I_{nn'}^{(5)}=2^{1/2}\int_0^1(\rho_0+x)R_n(\rho_0+x)R_{n'}(\rho_0+x)dx \tag{A13}$$

with $R_n(\rho)$ given by Eq. (8), n, $n'=1,2,\ldots$.

Since, in general, there is no a analytical expression of the integrals (A10)–(A13) in the literature,[37,38] we performed their direct numerical evaluation.

[1] B.J. van Wees, H. van Houten, C.W.J. Beenakker, J.G. Williamson, L.P. Kouwenhoven, D. van der Marel, and C.T. Foxon, Phys. Rev. Lett. **60**, 848 (1988).
[2] D.A. Wharam, T.J. Thornton, R. Newbury, M. Pepper, H. Ahmed, J.E.F. Frost, D.G. Hasko, D.C. Peacock, D.A. Ritchie, and G.A.C. Jones, J. Phys. C **21**, L209 (1988).
[3] C.S. Chu and R.S. Sorbello, Phys. Rev. B **40**, 5941 (1989).
[4] P.F. Bagwell, Phys. Rev. B **41**, 10 354 (1990).
[5] E. Tekman and S. Ciraci, Phys. Rev. B **42**, 9098 (1990).
[6] E. Tekman and P.F. Bagwell, Phys. Rev. B **48**, 2553 (1993).
[7] Y.S. Joe and R.M. Cosby, J. Appl. Phys. **81**, 6217 (1997).
[8] C.S. Kim, A.M. Satanin, Y.S. Joe, and R.M. Cosby, Phys. Rev. B **60**, 10 962 (1999); Zh. Éksp. Teor. Fiz. **116**, 263 (1999) [JETP **89**, 144 (1999)].
[9] R.L. Schult, D.G. Ravenhall, and H.W. Wyld, Phys. Rev. B **39**, 5476 (1989).
[10] P. Exner, Phys. Lett. A **141**, 213 (1989); P. Exner and P. Šeba, J. Math. Phys. **30**, 2574 (1989); P. Exner, P. Šeba, and P. Štovíček, Chech. J. Phys. B **39**, 1181 (1989); Phys. Lett. A **150**, 179 (1990); M.S. Ashbough and P. Exner, *ibid.* **150**, 183 (1990).
[11] J. Goldstone and R.L. Jaffe, Phys. Rev. B **45**, 14 100 (1992).
[12] D.W.L. Sprung, H. Wu, and J. Martorell, J. Appl. Phys. **71**, 515 (1992).
[13] F. Sols and M. Macucci, Phys. Rev. B **41**, 11 887 (1990).
[14] J.P. Carini, J.T. Londergan, K. Mullen, and D.P. Murdock, Phys. Rev. B **46**, 15 538 (1992).
[15] J.P. Carini, J.T. Londergan, K. Mullen, and D.P. Murdock, Phys. Rev. B **48**, 4503 (1993).
[16] K. Vacek, H. Kasai, and A. Okiji, J. Phys. Soc. Jpn. **61**, 27 (1992).
[17] F. Lenz, J.T. Londergan, E.J. Moniz, R. Rosenfelder, M. Stingl, and K. Yazaki, Ann. Phys. (N.Y.) **170**, 65 (1986).
[18] K.T. Tang, B. Kleinman, and M. Karplus, J. Chem. Phys. **50**, 1119 (1969).
[19] J.A. Cochran and R.G. Pecina, Radio Sci. **1**, 679 (1966).
[20] L. Lewin, D. C. Chang, and E. F. Kuester, *Electromagnetic Waves and Curved Structures* (Peter Peregrinus, Stevenage, UK, 1977).
[21] B. Z. Katsenelenbaum, L. Mercader del Río, M. Pereyaslavets, M. Sorolla Ayza, and M. Thumm, *Theory of Nonuniform Waveguides* (IEE, London, UK, 1998).
[22] C.P. Bates, Bell Syst. Tech. J. **49**, 2259 (1969).
[23] M. Jouguet, Ann. Telecommun. **2**, 78 (1947); Cables Transm. **1**, 39 (1947).
[24] M. Spivack, J. Ogilvy, and C. Sillence, Waves Random Media **12**, 47 (2002).
[25] R. Landauer, IBM J. Res. Dev. **1**, 223 (1957); Philos. Mag. **21**, 863 (1970).
[26] E.N. Bulgakov and A.F. Sadreev, Pis'ma Zh. Éksp. Teor. Fiz. **66**, 403 (1997) [JETP Lett. **66**, 431 (1997)]; Zh. Éksp. Teor. Fiz. **114**, 1954 (1998) [JETP **87**, 1058 (1998)].
[27] *Handbook of Mathematical Functions*, edited by M. Abramowitz and I. A. Stegun (Dover, New York, 1964).
[28] J.A. Cochran, J. Soc. Ind. Appl. Math. **12**, 580 (1964).
[29] K.-F. Berggren and Z.-L. Ji, Phys. Rev. B **47**, 6390 (1993).
[30] C.S. Lent, Appl. Phys. Lett. **56**, 2554 (1990).
[31] E. Jahnke, F. Emde and F. Lösch, *Tables of Higher Functions* (McGraw-Hill, New York, 1960).
[32] E. Bahar, IEEE Trans. Microwave Theory Tech. **17**, 210 (1969); E. Bahar and G. Govindarajan, *ibid.* **21**, 819 (1973).
[33] J. von Neumann and E. Wigner, Z. Phys. **30**, 465 (1929); F.H. Stillinger and D.R. Herrick, Phys. Rev. A **11**, 446 (1975); H. Friedrich and D. Wintgen, *ibid.* **31**, 3964 (1985); **32**, 3231 (1985).
[34] K. Okamoto, *Fundamentals of Optical Waveguides* (Academic, New York, 2000).
[35] E.A.J. Marcatili, Bell Syst. Tech. J. **48**, 2103 (1969).
[36] K. Thyagarajan, M.R. Shenoy, and A.K. Ghatak, Opt. Lett. **12**, 296 (1987).
[37] I. S. Gradshteyn and I. M. Ryzhik, *Table of Integrals, Series, and Products* (Academic, New York, 1980).
[38] A. P. Prudnikov, Yu. A. Brychkov, and O. I. Marichev, *Integrals and Series* (Gordon and Breach, New York, 1986), Vol. 2.